SCIENCE CHINA
Information Sciences

October 2021, Vol. 64 200301:1–200301:21
https://doi.org/10.1007/s11432-020-3261-5

• REVIEW •
Special Focus on Reconfigurable Intelligent Surfaces for Future Wireless Communications

Reconfigurable intelligent surfaces for smart wireless environments: channel estimation, system design and applications in 6G networks†

Ying-Chang LIANG*[1], Jie CHEN[1], Ruizhe LONG[1], Zhen-Qing HE[1], Xianqi LIN[2], Chenlu HUANG[2], Shilin LIU[2], Xuemin (Sherman) SHEN[3] & Marco Di RENZO[4]

[1]*Center for Intelligent Networking and Communications, University of Electronic Science and Technology of China, Chengdu* 611731, *China;*
[2]*School of Electronic Science and Engineering, University of Electronic Science and Technology of China, Chengdu* 611731, *China;*
[3]*Department of Electrical and Computer Engineering, University of Waterloo, Waterloo* N2L 3G1, *Canada;*
[4]*Université Paris-Saclay, CNRS, CentraleSupélec, Laboratoire des Signaux et Systèmes,* 3 *Rue Joliot-Curie,* 91192 *Gif-sur-Yvette, France*

Received 27 December 2020/Revised 22 April 2021/Accepted 12 May 2021/Published online 7 July 2021

Abstract Reconfigurable intelligent surface (RIS), one of the key enablers for the sixth-generation (6G) mobile communication networks, is considered by designers to smartly reconfigure the wireless propagation environment in a controllable and programmable manner. Specifically, an RIS consists of a large number of low-cost and passive reflective elements (REs) without radio frequency chains. The system gain of RIS wireless systems can be achieved by adjusting the phase shifts and amplitudes of the REs so that the desired signals can be added constructively at the receiver. However, an RIS typically has limited signal processing capability and cannot perform active transmitting/receiving in general, which leads to new challenges in the physical layer design of RIS wireless systems. In this paper, we provide an overview of the RIS-aided wireless systems, including the reflection principle, channel estimation, and system design. In particular, two types of emerging RIS systems are considered: RIS-aided wireless communications (RAWC) and RIS-based information transmission (RBIT), where the RIS plays the role of the reflector and the transmitter, respectively. We also envision the potential applications of RIS in 6G networks.

Keywords reconfigurable intelligent surface, channel estimation, RIS-aided wireless communications, RIS-based information transmission, 6G

Citation Liang Y-C, Chen J, Long R Z, et al. Reconfigurable intelligent surface for smart wireless environment: channel estimation, system design and applications in 6G networks. Sci China Inf Sci, 2021, 64(10): 200301, https://doi.org/10.1007/s11432-020-3261-5

1 Introduction

With the wide deployment of the fifth-generation (5G) mobile communication systems, it is now a critical time to develop enabling technologies for the sixth-generation (6G) communication systems. Overall, 6G systems are expected to fulfill more stringent requirements on transmission capacity, reliability, latency, coverage, energy consumption, and connection density [1–4]. The existing techniques in 5G, such as millimeter-wave (mmWave) communications, massive multi-input multi-output (MIMO), ultra-dense heterogeneous networks, mainly focus on the system design at the transmitter and receiver sides, the purpose of which is to cope with the unfavorable wireless propagation environment. Recently, reconfigurable intelligent surface (RIS), also called intelligent reflecting surface, has emerged as a promising technology for its capability of configuring a wireless propagation environment [5–19]. Such technology provides designers with additional degrees of freedom to fulfill the stringent requirements of 6G.

* Corresponding author (email: liangyc@ieee.org)
† Invited article

In particular, an RIS is a two-dimensional array with a large number of reflective elements (REs), each of which can appropriately reflect the incident electromagnetic wave. Hence, by smartly adjusting the reflection coefficients of the REs with a programmable controller, the reflected signals can propagate in a desired way towards the intended receivers. As a result, the wireless environment becomes controllable and programmable. Specifically, an RIS can be utilized to implement two promising communication paradigms, i.e., RIS-aided wireless communications (RAWC) and RIS-based information transmission (RBIT).

In RAWC, the RIS acts as a reflector to realize the desired signal combination or interference cancellation at the intended receivers, thereby assisting the existing transmissions with higher spectrum-/energy-efficiency. Compared with existing amplify-and-forward (AF) relay aided communications [14,20,21], RIS is a more energy-/cost-efficient technique, because the RIS reflects the incident signals passively without requiring power-consuming radio frequency (RF) components, i.e., converters and oscillators.

In RBIT, the RIS acts as an information transmitter and modulates its own messages over the existing modulated or unmodulated RF radio wave generated by other devices [22,23]. By proactively varying the reflection coefficients of the RIS-based on specific reflection patterns, the intended receiver can detect these artificial variations and decode the embedded messages encoded by the RIS. Compared with conventional backscatter communications [24–28], the use of an extremely large number of REs at the RIS helps to enhance the desired RF source, and greatly improves the performance of backscatter communications [29]. Moreover, the collaboration between the RIS information transmission and active primary transmission yields mutually beneficial spectrum and energy sharing, and such system is also termed symbiotic radio (SR) [29,30].

RIS builds a controllable and software-defined wireless environment, and extends the frontiers of wireless communication design, offering novel solutions to 6G. For its promising capability, there have been intensive research activities on RIS in the past few years, and several tutorials and survey papers have appeared in the literature. Specifically, the review paper [5] provides an overview of the reflection basics and implementations of RIS, and it also introduces the technology evolving path of various reflection-based radio technologies including reflective array, backscatter communications, ambient backscatter, and RIS. The review paper [6] provides the antenna design, prototyping, and experimental results of RIS, and the review papers [7–13] provide an overview of RIS technology and its applications in typical wireless communication scenarios. The survey paper [14] is focused on the differences and similarities between relays and RISs. The tutorial papers [15–17] are focused on channel modeling and theoretical performance evaluation of RIS-assisted wireless communication systems. The survey papers [18,19] consider the application of deep learning to achieve channel estimation, signal detection, and beamforming optimization in RAWC.

There are various challenges when deploying RISs into wireless communication systems since RISs have limited signal processing capability and cannot perform active transmitting/receiving in general. Differently from previous studies [5–19] that are focused on RIS implementation, prototyping, and applications, this paper provides a different perspective. Specifically, we focus on the main state-of-the-art techniques to solve fundamental problems at the physical layer and for deploying RISs into wireless communication systems, such as channel estimation, joint active and passive beamforming optimization for the system design of RAWC, and passive information transmission optimization for the system design of RBIT. Besides, we envision related potential research directions for the deployment of RISs for 6G.

The rest of this paper is organized as follows: Section 2 introduces an overview of the RIS system. Then, Section 3 presents the channel estimation problem and shows the corresponding main solutions. Section 4 discusses the joint active and passive beamforming optimization for RAWC. In Section 5, we present passive information transmission optimization for RBIT. Finally, Section 6 discusses the potential applications of RISs in 6G networks and Section 7 concludes the paper. By the way, the list of abbreviations of this paper is given in Table 1.

2 RIS in communication systems

In this section, we first introduce the basic system models of two communication paradigms with RISs and then investigate the reflection principle of RISs.

Table 1 List of abbreviations

Abbreviation	Description	Abbreviation	Description
5G	Fifth-generation	6G	Sixth-generation
ADC	Analog-to-digital converters	AF	Amplify-and-forward
AoA	Angle of arrival	AO	Alternating optimization
AoD	Angle of departure	BS	Base station
Big-AMP	Bilinear generalized approximate message passing	CSI	Channel state information
BSUM	Block successive upper-bound minimization	CR	Cognitive radio
CRLB	Cramér-Rao lower bound	DAC	Digital-to-analog converters
DCCE	Direct cascaded channel estimation	DFT	Discrete Fourier transform
DnCNN	Denoising convolutional neural network	DRL	Deep reinforcement learning
SCCE	Seperate cascaded channel estimation	ELPC	Extremely low-power communication
ERLLC	Extremely reliable and low-latency communications	FeMBB	Further-enhanced mobile broadband
FPGA	Field-programmable gate array	IoT	Internet-of-Things
KPI	Key performance indicator	LS	Least-square
MEC	Mobile edge computing	MISO	Multi-input single-output
MEMS	Microelectromechanical system	MCU	Micro-controller unit
MMSE	Minimum mean-squared-error	MINLP	Mixed-integer non-linear program
MIMO	Multi-input multi-output	mmWave	Millimeter-wave
NOMA	Non-orthogonal multiple access	OFDM	Orthogonal frequency division multiplexing
PARAFAC	Parallel factor	PIN	Positive-intrinsic-negative
PGM	Projected gradient method	PSK	Phase shift-keying
PCB	Printed circuit board	QAM	Quadrature amplitude modulation
RAWC	RIS-aided wireless communications	RHCP	Right-handed circularly polarized
RBIT	RIS-based information transmission	RE	Reflective element
RIS	Reconfigurable intelligent surface	RCO	Reflection coefficient based optimization
SINR	Signal-to-interference-plus-noise ratio	SPC	Short packet communication
SWIPT	Simultaneous wireless information and power transfer	SDR	Semidefinite relaxation
SR	Symbiotic radio	SSCA	Stochastic successive convex approximation
SNR	Signal-to-noise ratio	THz	Terahertz
umMTC	Ultra-massive machine-type communication	UC	Upper computer
USRP	Universal software radio peripheral	VLC	Visible light communications

2.1 System models

An RIS is generally regarded as a nearly-passive device, which has to leverage the existing active radio waves to operate its function. Specifically, the system models with RISs are shown in Figure 1, which are mainly composed of two channels, namely the direct-link channel and the RIS-related channel. The transmitter generates an active signal to send its messages to the receiver via the direct-link channel and the RIS-related channel, while the RIS varies its reflection coefficient matrix via the RIS-related channel according to the following two communication paradigms.

In Figure 1(a), the RIS attempts to provide additional channel diversity via the RIS-related link, and the existing active transmission is therefore successfully performed even if the direct-link is blocked due to obstacles. Moreover, by properly designing the reflection coefficient matrix according to the instantaneous and/or statistical channel state information (CSI), the signal transmission can be enhanced thanks to the phase alignment of the reflected signal, which is referred to as RAWC.

In Figure 1(b), the RIS is enabled to send its own messages to the potential receiver by appropriately varying its reflection coefficients periodically, and the receiver can decode the messages from the RIS-related channel by detecting the signal variations, which is referred to as RBIT.

We evince that RIS-based communications rely on the design of the reflection coefficients, it is therefore important to understand how to practically realize the tunable reflection coefficients.

2.2 Reflection principle

In electromagnetic theory, a reflection occurs when the radio wave reaches the interface between two different media, and some part of the radio wave returns into the medium from which it is originated. For example, the reflection in RIS-aided systems occurs when the incident signal from the transmitter

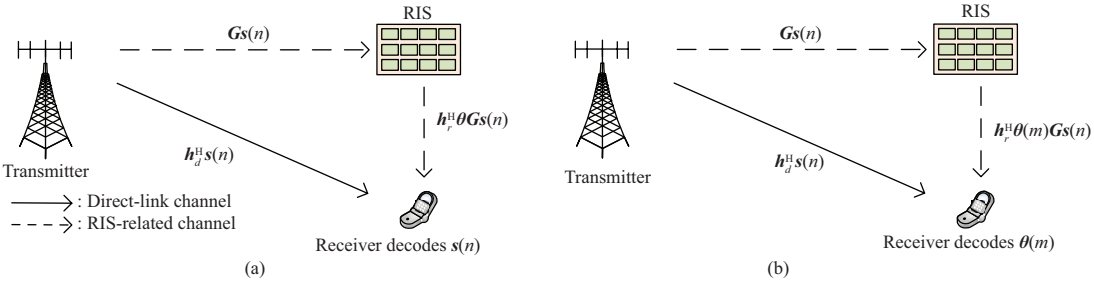

Figure 1 (Color online) Two communication paradigms of RIS. (a) RAWC; (b) RBIT. The RIS in (a) assists the transmitter to deliver $\boldsymbol{s}(n)$ to the receiver by adjusting its reflection coefficient matrix $\boldsymbol{\theta}$ according to the CSI, while the RIS in (b) delivers its own message to the receiver by proactively varying its reflection coefficient matrix $\boldsymbol{\theta}(m)$. The receiver in (a) aims to decode the messages embedded in $\boldsymbol{s}(n)$, while the receiver in (b) aims to decode the messages embedded in $\boldsymbol{\theta}(m)$ and possible $\boldsymbol{s}(n)$ depending on its decoding strategy. The transmitter-receiver, transmitter-RIS, and RIS-receiver channels are denoted by $\boldsymbol{h}_d^{\mathrm{H}}$, $\boldsymbol{G}$, and $\boldsymbol{h}_r^{\mathrm{H}}$ (the superscript H denotes the conjugate transpose operation), respectively.

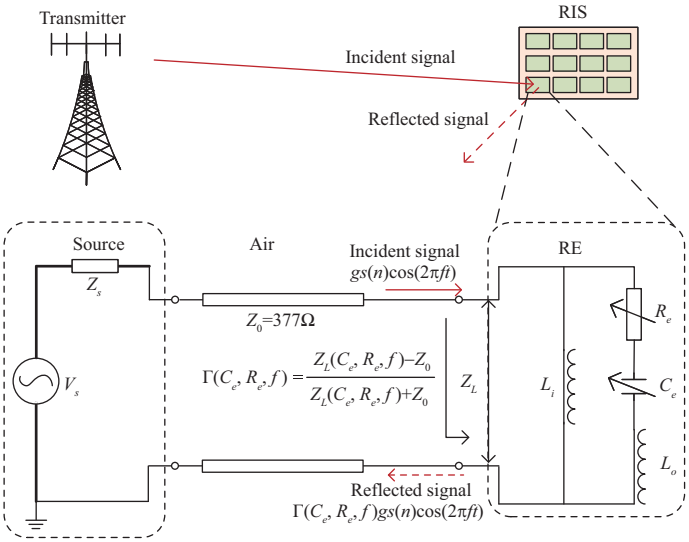

Figure 2 (Color online) The equivalent circuits for the RIS reflecting element based on transmission line theory.

encounters each RE at the RIS. To precisely characterize the reflected signal, it is necessary to solve Maxwell's equations by applying the boundary conditions at the interface of different media by taking into account the permittivity and permeability of the REs [31–33]. However, the calculation of Maxwell's equations is non-trivial and some simplifications are needed. In wireless engineering, when the physical size of an RE is smaller than the wavelength of the incident signal, transmission line theory is considered as an adequate simplification of Maxwell's equations by using effective parameters [12]. The reflection coefficient is adopted to illustrate the ratio between the input and output electric fields. As shown in Figure 2, the reflection coefficient is characterized by the characteristic impedance Z_0 and the load impedance Z_L. Specifically, the characteristic impedance is a fixed value determined by the geometry and materials of the transmission line. As for the REs in the RIS, the air is regarded as the invisible transmission line with $Z_0 = 377\ \Omega$, whereas the load impedance is a reconfigurable value determined by the load circuit design. This provides a method to realize the tunable reflection coefficient by varying the load impedance.

The simplest way to change the reflection coefficients is to deploy a switch on a set of preset load impedances, which is common in backscatter communication and low-resolution RIS. However, as the RIS has to cater to the CSI with all phase shifts as much as possible, it is highly desirable to continuously vary the phase shifts of the REs. Considering a printed circuit board (PCB)-based RIS with uniformly distributed REs on a planar surface, the RIS embeds a semiconductor, typically a positive-intrinsic-negative (PIN) diode, into the metal element in the outer layer to tune the reflection coefficients [34]. Within a given biasing voltage range, the PIN diode can be replaced with the equivalent circuit model shown in Figure 2, where C_e and R_e are the effective capacitance and resistance, respectively. As such,

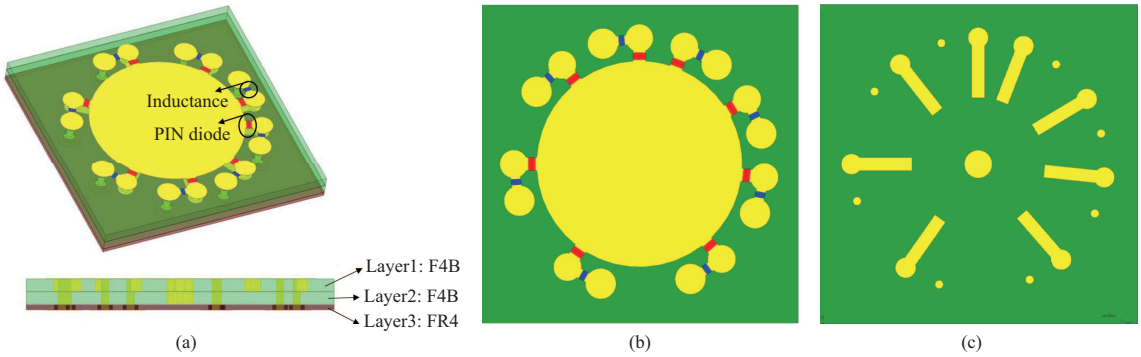

Figure 3 (Color online) Structure of the RE. (a) Overall view of the RE; (b) top view of Layer1; (c) top view of Layer2.

the load impedance is determined by

$$Z(C_e, R_e, f) = \frac{\mathrm{j}2\pi f L_i(\mathrm{j}2\pi f L_o + \frac{1}{\mathrm{j}2\pi C_e} + R_e)}{\mathrm{j}2\pi f L_i + \mathrm{j}2\pi f L_o + \frac{1}{\mathrm{j}2\pi C_e} + R_e}, \tag{1}$$

where L_i, L_o, and f denote the inner layer inductance, the outer layer inductance, and the carrier frequency, respectively. Notice that the load impedance is a function of the variables C_e, R_e, and f. By varying the biasing voltage of the PIN, the load impedance is adjusted by varying its effective capacitance continuously. Consequently, the reflection coefficient can be varied continuously. However, such a design also introduces additional constraints on the reflection response. That is, the amplitude and phase cannot be independently varied [34].

2.3 An implementation of RIS

There exist several methods proposed to reconfigure the reflection coefficients, such as loading PIN diodes [35–44], varactor diodes [45–47], and microelectromechanical system (MEMS) switches [48–50]. A PIN loaded RE was presented in [35], where the PIN can be switched between its ON or OFF state to reverse the reflection phase, thus achieving 1-bit phase quantization. A varactor diode was adopted in [46, 47] to achieve a continuous reflection phase shift. Specifically, in [47], an RE loaded with four varactor diodes was proposed where the reflection phase can be changed continuously over 360° by controlling the biasing voltages of the varactor diode through the digital-to-analog converters (DACs) module. In addition, when the operating frequency is in the millimeter-wave band, the MEMS switches become a promising alternative to the PIN diodes, since the latter may introduce larger insertion losses. Moreover, REs loaded with liquid crystal [51, 52] and graphene [53, 54] also exhibit good performance.

To dynamically control the RIS, a system based on a micro-controller unit (MCU) [41], DACs board [45–47], and field-programmable gate array (FPGA) [55–59] are usually used. In [56], the RIS is composed of 32×8 REs, each of which is loaded with two varactor diodes to achieve a reflection phase range of 450°. Then, a central controller, FPGA, and DAC are utilized to generate bias voltage to tune the varactor for the desired phase distribution. The signal is then loaded on the carrier when the incident wave is reflected by the RIS. Finally, a universal software radio peripheral (USRP) can be used to demodulate the received signal.

Although the REs can realize a continuous reflection phase by using varactors, the introduced amplitude loss is higher than that of PIN-loaded REs. Nevertheless, the REs loaded with PIN diodes discussed above realize at most 2-bit phase quantization. Moreover, existing REs mainly work on linear polarization, and relatively few research studies are found on circular polarization RE with a tunable reflection phase. Huang [60] proposed an RE composed of a rectangular patch and phase delay line, where the reflection phase can change with the length of the phase delay line. Based on this working principle, we propose a circularly polarized RIS with a 3-bit reconfigurable reflection phase in the range of 0°∼360°. As shown in Figure 3, PIN diodes are loaded between the circular patch and each phase delay line, where the reflection phase can be controlled by switching the ON-OFF state of the PIN diodes. The bias circuit of each RE is composed of eight inductors, each of which is connected to eight phase delay lines (see Figure 3(c)), thus the quantization accuracy of the reflected phase is 45°. In addition, we model the proposed RE in the CST studio suite to verify its performance. By setting the right-handed circularly polarized (RHCP)

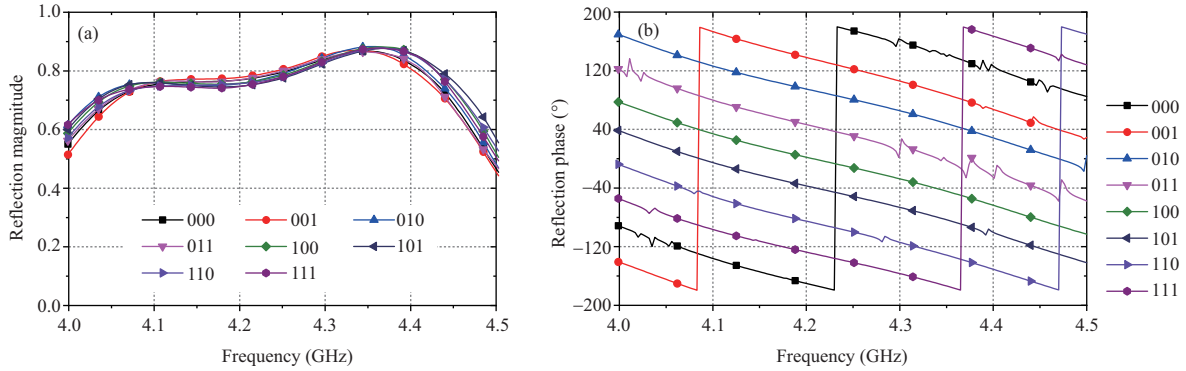

Figure 4 (Color online) Simulated magnitude and phase response of the RE. (a) Reflection magnitude response of the RE; (b) reflection phase response of the RE.

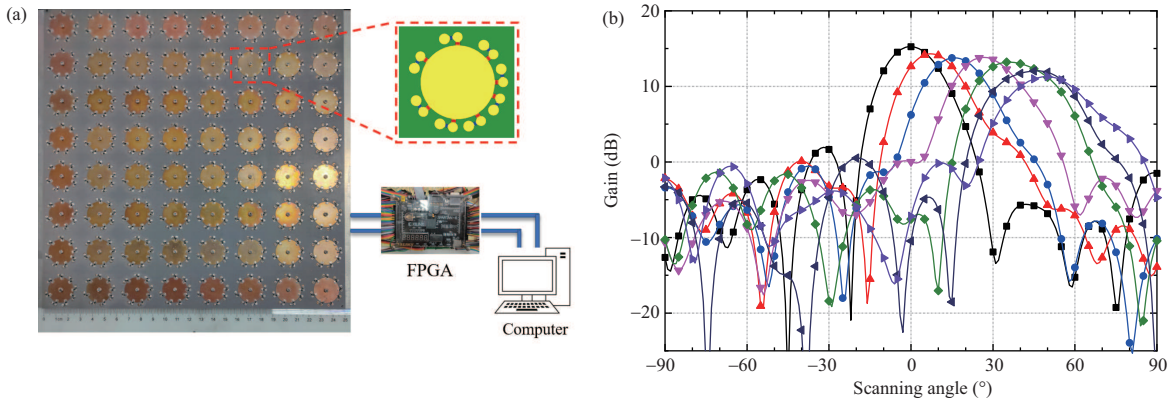

Figure 5 (Color online) Structure of the RIS and its radiation performance. (a) Structure of the RIS; (b) radiation patterns of reflected beam scanning.

plane wave incidence condition and unit cell boundary conditions, the simulated reflection magnitude and phase responses of the RE are illustrated in Figure 4. Specifically, Figure 4(a) shows that the reflection magnitude of the RE is greater than 0.75 within the range of 4.1∼4.44 GHz, and Figure 4(b) shows that a good linearity of the phase response can be obtained under various working states, which is beneficial for the design of a wide-band RIS.

Then, as shown in Figure 5(a), an RIS consisting of 8×8 of the above designed REs is obtained, resulting in an aperture size of 248 mm×248 mm. To steer the signal from the incident beam direction $(\theta_{\rm inc}, \varphi_{\rm inc})$ towards a reflected radiation beam pointing to (θ_m, φ_m), the required phase compensation at the n-th RE is [61]

$$\phi_n = -\frac{2\pi}{\lambda}[x_n\left(\sin\theta_m\cos\varphi_m - \sin\theta_{\rm inc}\cos\varphi_{\rm inc}\right) + y_n\left(\sin\theta_m\sin\varphi_m - \sin\theta_{\rm inc}\sin\varphi_{\rm inc}\right)], \tag{2}$$

where λ is the free-space wavelength at the center frequency and (x_n, y_n) is the position of the n-th RE.

In the considered RIS, the reflection phase of each RE is controlled by an upper computer (UC) through FPGA. Specifically, the UC first codes the designed quantized phase, and then sent it to the FPGA which connects the PIN diodes on the RIS by its output pin. Then, each PIN diode loaded on the RE is switched to the ON or OFF states to get the desired phase distribution. Thus, the reflected radiation pattern can be reconfigured dynamically with different codes sent to the FPGA. Based on this control method, the simulated radiation pattern of beam scanning is shown in Figure 5(b), which provides a peak gain of 15.6 dB in the broadside and a beam scanning range of 50°. The simulated result verifies the excellent performance of the designed 3-bit circularly polarized RIS.

3 Channel estimation for RIS-assisted systems

CSI acquisition is one of the main challenges for the deployment of RIS-assisted systems. This is because the joint design of active beamforming at the transceiver and passive beamforming (reflection coefficient matrix) at the RIS requires the CSI of the corresponding wireless links.

In this section, we briefly introduce the fundamental channel estimation problems of RIS-assisted systems. Then, we overview state-of-the-art channel estimation methods. Moreover, we investigate the pros and cons of two main channel estimation methods, namely the separate and direct channel estimations, and depict their applicable scenarios, respectively.

3.1 Cascaded channel model

Channel estimation in RIS-assisted systems is more challenging than in traditional active devices based MIMO systems. This is due to the following reasons. Firstly, CSI acquisition in active device based systems can be achieved directly by sending training sequences. As for RIS-assisted systems, the channel estimation can only be performed at the active transceivers, since the RIS is a passive device without active transmitting/receiving capabilities. Secondly, an RIS is usually equipped with a large number of REs, thereby causing a high training overhead. Finally, it is quite difficult to recover the CSI of the transmitter-RIS channel and RIS-receiver channel separately, because they are coupled together with the reflection coefficient matrix. To tackle the above challenges, researchers conducted research to find innovative methods to estimate the cascaded channel, which accounts for the transmitter-RIS channel and RIS-receiver channel.

As an example, we illustrate a typical scenario to explain the reason why it is sufficient to acquire the cascaded channels, rather than the individual transmitter-RIS and RIS-receiver channels, for the passive beamforming design in RIS-assisted systems. Specifically, we consider an RIS-assisted multi-user MISO system, where the base station (BS) is equipped with M antennas to serve K single-antenna and the RIS is equipped with L REs. Denote the channel responses from the BS to the RIS, from the RIS to the k-th user, and from the BS to the k-th user by $\boldsymbol{G} \in \mathbb{C}^{L\times M}$, $\boldsymbol{h}_{r,k} \in \mathbb{C}^{L}$, and $\boldsymbol{h}_{d,k} \in \mathbb{C}^{M}$, respectively. Then, the combined channel response from the BS to the k-th user is given by [62, 63]

$$\boldsymbol{h}_{d,k}^{\mathrm{H}} + \boldsymbol{h}_{r,k}^{\mathrm{H}}\mathrm{diag}(\boldsymbol{v})\boldsymbol{G} = \boldsymbol{h}_{d,k}^{\mathrm{H}} + \boldsymbol{v}^{\mathrm{T}}\mathrm{diag}(\boldsymbol{h}_{r,k}^{\mathrm{H}})\boldsymbol{G}, \tag{3}$$

where $\mathrm{diag}(\boldsymbol{v}) \in \mathbb{C}^{L\times L}$ is the diagonal reflection coefficient matrix to be designed. We observe from the second term of the right hand side of (3) that the design of the passive reflection coefficients, i.e., $\boldsymbol{v}$, only requires the CSI of the direct-link $\boldsymbol{h}_{d,k}$ and the following cascaded channel:

$$\boldsymbol{H}_k = \mathrm{diag}(\boldsymbol{h}_{r,k}^{\mathrm{H}})\boldsymbol{G}, \tag{4}$$

which has a bilinear structure in unknown $\boldsymbol{h}_{r,k}^{\mathrm{H}}$ and $\boldsymbol{G}$.

Note that the direct-link $\boldsymbol{h}_{d,k}$ can be estimated by setting two proper reflection coefficient matrices, i.e., arbitrary $\mathrm{diag}(\boldsymbol{v}_1)$ and $\mathrm{diag}(\boldsymbol{v}_2) = -\mathrm{diag}(\boldsymbol{v}_1)$ in the first and second training slots, respectively. Then, the reflection impacts of RIS can be canceled by summarizing the received two training signals, i.e.,

$$\boldsymbol{h}_{r,k}^{\mathrm{H}}\mathrm{diag}(\boldsymbol{v}_1)\boldsymbol{G} + \boldsymbol{h}_{r,k}^{\mathrm{H}}\mathrm{diag}(-\boldsymbol{v}_1)\boldsymbol{G} = \boldsymbol{0}. \tag{5}$$

This indicates that the CSI of the direct-link can be estimated by using traditional MIMO channel estimation methods.

Based on the above discussion, the main challenge for the CSI acquisition in RIS-assisted systems lies in the cascaded channel estimation and much effort has been invested in this direction. Generally, the state-of-the-art cascaded channel estimation methods can be divided into two categories: the separate cascaded channel estimation (SCCE) and the direct cascaded channel estimation (DCCE).

3.2 Separate cascaded channel estimation

In this subsection, we introduce the SCCE method, which acquires the CSI of the BS-RIS channel and the RIS-user channel from the received training signals, respectively, and uses the associated two channels to reconstruct the cascaded channels.

3.2.1 *SCCE for semi-passive RIS*

One straightforward method to estimate the BS-RIS channel and the RIS-user channel is to insert some active sensors among the passive REs [64] at the RIS, which is referred to as the semi-passive RIS. In [64], channel sparsity is assumed for the BS-RIS channel and RIS-user channel, i.e., both of them consist of a few physical transmission paths and each path involves one scalar path-loss and one angle of arrival/departure (AoA/AoD) steering vector. Then, the BS or the users transmit pilot sequences successively to the active sensors of the RIS to estimate the angles and path loss of the BS-RIS channel or RIS-user channels. Based on this method, the CSI from the transmitter to the passive REs can be recovered from the estimated CSI from the transmitter to the active sensors by using, e.g., compressive sensing and deep learning methods.

The above method only needs a few training signals to estimate the CSI associated with a small number of active sensors, which is sufficient to recover the full CSI with a large number of passive REs, thereby reducing the overall training overhead. However, there exist some drawbacks in the semi-passive RIS scheme. First, the full CSI is recovered by capitalizing on the correlated channel impulse responses between the REs and the active sensors, which cannot be applicable to the cases of uncorrelated channels, e.g., the Rayleigh fading channels. Second, the deployment of active sensors increases the hardware/energy cost and signal processing complexity. Moreover, the estimated CSI needs to be fed back to the BS and the users for the joint active and passive beamforming design, which decreases the transmission efficiency.

3.2.2 *SCCE for full-passive RIS*

To tackle the limitations of the semi-passive RIS scheme, SCCE methods for full-passive RIS are further investigated in [65–70] without introducing any active sensors.

For an RIS-aided single-user MIMO system, a two-stage channel estimation method was proposed in [65, 66], where the user transmits training sequences to the BS through RIS with different reflection coefficient matrices. In this type of method, the received signals are rewritten as an affine bilinear matrix factorization form, i.e., the product of the RIS-BS channel matrix, the user-RIS channel matrix, and the training pilot matrix. In [65], the BS-RIS channel was estimated by iteratively solving a fixed point equation in the first stage and the RIS-user channel was obtained by using the least-square (LS) estimator in the second stage. In [66], the low-rankness of the RIS-user channel matrix was further considered to reduce the training overhead. Particularly, in the first stage, the BS-RIS channel and the product-matrix of the user-RIS channel and the training pilots were recovered from the received signals by applying the bilinear generalized approximate message passing (BiG-AMP) algorithm for matrix factorization. In the second stage, the RIS-user channel was recovered from the product-matrix by applying a Riemannian manifold gradient-based algorithm for matrix completion.

The channel estimation problems for RIS-aided multi-user MIMO systems were further considered in [67–70]. Specifically, in [67] a matrix-calibration based matrix factorization problem was formulated under the assumption of channel sparsity, and an iterative Bayesian inference algorithm was derived to estimate BS-RIS channel and RIS-user channels, respectively. In [68], the anchor-assisted two-phase channel estimation scheme was developed, where two anchor nodes were deployed near the RIS to help the channel estimation. Particularly, in the first phase, the two deployed anchor nodes transmit pilots successively to estimate the square of the element-wise BS-RIS channel gain. In the second phase, the obtained partial knowledge of the BS-RIS channel is further used to estimate RIS-user channels. The anchor-assisted channel estimation method is efficient for RIS-assisted massive access systems since such partial knowledge is common to all users. In [69], the parallel factor (PARAFAC) decomposition based scheme was investigated, where the PARAFAC was applied to factorize the high dimensional tensor into a linear combination of multiple rank-one tensors and the alternating LS was used to recover the unknown channels from the decomposed tensors.

The SCCE methods in [65–70] assume sparse, low-rank, or quasi-static channel properties when performing channel estimation. In addition, the inaccurate BS-RIS channel and RIS-user channel estimation in the SCCE methods will produce reconstruct error when recovering the cascaded channels. This degrades the cascaded channel estimation performance.

3.3 Direct cascaded channel estimation

In this subsection, we introduce the DCCE method, which estimates the cascaded channels directly with a properly designed channel estimation protocol.

3.3.1 *Binary reflection based DCCE*

One straightforward method to estimate the cascaded channel directly is to turn on only one RE and keep the remaining REs off in each training slot. This method is referred to as the binary reflection method, which was initially proposed in [71] for an RIS-assisted single-user system. Then, a sub-group based binary reflection was further investigated in [72] for an RIS-assisted orthogonal frequency division multiplexing (OFDM) systems. In this scheme, REs are divided into multi sub-groups and each sub-group consisting of adjacent elements shares a common reflection coefficient. Due to spatial correlation, the cascaded channels of the REs in the same sub-group can be estimated together by applying binary reflection methods.

However, the training overhead in the binary methods scales with the number of REs (or sub-groups), which needs a large training overhead. Besides, the binary reflection method suffers from the low power gain of the reflected signals since only one RE (or one sub-group REs) works and the rest REs keep turned off in the binary reflection method.

3.3.2 *Full reflection based DCCE*

To tackle drawbacks of large training overhead and low reflected signal power in binary reflection based method, full reflection based DCCE method was further proposed in [73] based on minimizing the Cramér-Rao lower bound (CRLB), where all REs keep turned on in the whole training duration and the training reflection coefficients are designed as a discrete Fourier transform (DFT) matrix. By using the similar grouping idea in [72] to reducing training overhead, the method in [73] was further extended to an RIS-aided OFDM single-user system with or without considering the Doppler effect in [74, 75], respectively. Based on the minimum mean-squared-error (MMSE) criterion, a deep learning based denoising convolutional neural network (DnCNN) was proposed in [76, 77] to perform DCCE, where the noisy LS channel estimation and a cleaned channel matrix are the input and output, respectively.

3.3.3 *Multi-user joint DCCE*

For a multi-user scenario, the cascaded channels of different users are correlated due to the common BS-RIS channel, which can be applied to design a multi-user joint channel estimator to improve the estimation performance and reduce the training overhead, especially for RIS-assisted massive access systems.

One straightforward method using the channel correlations is to apply the cascaded channel of an arbitrary user to represent the cascaded channels of the remaining users [78–80]. For example, without loss of generality, we can use the cascaded channel of the first user, i.e., $\boldsymbol{H}_1$, to represent the cascaded channels of the k-th user, i.e.,

$$\boldsymbol{H}_k = \underbrace{\operatorname{diag}\left(\boldsymbol{h}_{r,k}^{\mathrm{H}}\right)\operatorname{diag}\left(\boldsymbol{h}_{r,1}^{\mathrm{H}}\right)^{-1}}_{\boldsymbol{\Omega}_k}\underbrace{\operatorname{diag}\left(\boldsymbol{h}_{r,1}^{\mathrm{H}}\right)\boldsymbol{G}}_{\boldsymbol{H}_1} = \boldsymbol{\Omega}_k\boldsymbol{H}_1, \tag{6}$$

where $\boldsymbol{\Omega}_k$ is a diagonal matrix. As can be seen from (6), we only need to estimate the diagonal matrix $\boldsymbol{\Omega}_k$ if the common part $\boldsymbol{H}_1$ is given. Since the number of unknown parameters in $\boldsymbol{\Omega}_k$ is much smaller than that in $\boldsymbol{H}_k$, the estimation of $\boldsymbol{\Omega}_k$ is much easier than that of $\boldsymbol{H}_k$ and the training overhead can be reduced.

Specifically, by using the channel correlation in (6), a sequential estimation method was applied in [78] for a narrow-band communication system and in [79] for a wide-band communication system. In this method, the cascaded channel of one typical user was first estimated, and then the cascaded channels of the rest users are recovered successively by estimating the diagonal matrix $\boldsymbol{\Omega}_k$. Moreover, for a mmWave communication system, in [80] the channel correlation in (6) was exploited to represent the cascaded channels of all users with a common row-column-block sparsity structure. Then, the joint multi-user cascaded channel estimation problem was formulated as a sparse matrix recovery problem. This problem was solved by a two-step procedure consisting of subspace projection and iteratively reweighted optimization.

4 RIS-aided wireless communications

In RAWC, the RIS acts as a reflector that passively steers the incident signals towards a desired direction by adjusting the programmable reflection coefficients, thereby achieving signal enhancement or interference cancellation for various key performance indicators (KPIs). In this section, we briefly review the system design of the joint active beamforming at the transceiver and passive beamforming (reflection coefficient matrix) at the RIS in RAWC.

4.1 System design under ideal case

In this subsection, we consider the system design of joint active and passive beamforming under ideal cases, e.g., perfect CSI and continuous phase shifts. In fact, one of the main challenges of the system design under ideal cases is that the active and passive beamformers are coupled with each other in the objective/constraints. In general, the optimization problems of the joint active and passive beamforming are non-convex and difficult to solve. In the following, we will illustrate the state-of-the-art solutions to these problems.

4.1.1 *Reflection coefficient based optimization*

This reflection coefficient based optimization (RCO) method is motivated by the fact that the optimal active beamformer at the transceiver has a closed-form solution when the passive beamformer (reflection coefficient matrix) is fixed. By substituting this closed-form solution into the original problem, the reformulated problem only involves the passive beamformer and is relatively easy to solve. Specifically, the RCO method was applied for a single-user MISO system in [63] to solve the transmit power minimization problem, where the semidefinite relaxation (SDR) technique was further used to obtain the solution of the passive beamformer. Then, the RCO method was further extended to solve a minimum signal-to-interference-plus-noise ratio (SINR) maximization problem in a multi-user MISO system [81], where the optimal passive beamformer was obtained by assuming rank-one transmitter-RIS channel. However, the closed-form solution of the active beamformer required in the RCO method cannot be generally achieved in a complicated wireless communications system.

4.1.2 *Alternating optimization method*

To tackle the limitation in the RCO method, most of the literature applies alternating optimization (AO) method to solve the formulated non-convex problem, where the active and passive beamformers are alternatively optimized in two independent subproblems and each subproblem can be solved efficiently. Specifically, the AO method has been widely used to solve the spectrum efficiency or energy efficiency maximization for a multi-user MISO system [82, 83], non-orthogonal multiple access (NOMA) system [84, 85], cognitive radio (CR) system [86], physical layer security [62, 87–92], active RIS-aided networks [93], wireless powered communication networks [94], and simultaneous wireless information and power transfer (SWIPT) systems [95]. Despite being easy to implement, the AO approach updates a block of variables alternatively in each iteration, which usually requires a large number of iterations to guarantee convergence, especially for high-dimension optimization variables.

4.1.3 *Projected gradient method*

To address the slow convergence in the AO method, the projected gradient method (PGM) was proposed in [96, 97] for solving the capacity maximization problem. Specifically, the optimized active and passive beamformers simultaneously move in the gradient direction of the objective iteratively. Then, the resulting solutions are projected onto the feasible region if they lie outside of the feasible set before the next iteration. This method optimizes all variables in each iteration, resulting in a faster convergence and lower computational complexity than those in the AO method.

4.1.4 *Deep reinforcement learning based method*

Beside the above methods, deep reinforcement learning (DRL) based methods have attracted much attention to solve the joint active and passive beamformer design problems. In this method, by observing the predefined rewards with state and action spaces, the joint design of active and passive beamforming is optimized through trial-and-error interactions with the environment. Specifically, DRL based methods

were applied in the RIS-aided multi-user systems to solve spectrum-efficiency optimization problem in [98], secure capacity optimization problem in [99], energy-efficiency optimization problem in [100], and the Terahertz communication in [101].

4.2 System design under hardware constraints

In this subsection, we review the system design for the RAWC under practical hardware constraints, i.e., discrete phase shifts, phase-dependent amplitude variation, and transmit/receive signal distortion.

4.2.1 *Discrete phase shifts*

Continuous phase shift requires infinite bits to control each RE which requires high hardware and energy cost. In addition, the discrete phase shifts [102] will introduce misalignment of the interested signal at the intended receivers and result in performance degradation. This motivates us to consider the discrete phase shifts in the system design. However, the formulated problem by considering discrete phase shift is a mixed-integer non-linear program (MINLP) problem, which is NP hard and difficult to solve in general. To tackle this issue, the branch-and-bound method and AO method were used in [103] to minimize the total transmit power by considering discrete phase shift for a single-user case and multi-user case, respectively. In addition, a new penalized Dinkelbach block successive upper-bound minimization (BSUM) method was proposed in [104] to solve the rate maximization problem for an RIS-aided single-user MISO system.

4.2.2 *Phase-dependent amplitude variation*

The amplitude of the reflection coefficient is dependent on the phase shift of the incident wave in practice, which is minimum with zero phase shift and monotonically increases to approach unity amplitude with phase shift π or $-\pi$ [34]. This is because when the phase shift approaches zero, the image currents are in-phase with the reflecting element currents, thereby enhancing the electric field and the current flow in each RE. Then, the increased dielectric loss, metallic loss, and ohmic loss cause more energy consumption and lower reflection amplitude [105]. Specifically, the approximated partial power loss on the reflection amplitude $|\theta_n|$ of the n-th RE can be written as the function of its phase shift $\angle\theta_n$ [106], i.e.,

$$|\theta_n| = (1 - |\theta|_{\min}) \left(\frac{\sin(\angle\theta_n - \phi) + 1}{2} \right)^{\alpha} + |\theta|_{\min}, \tag{7}$$

where $|\theta|_{\min}$, ϕ, and α are constants related to the specific circuit implementation.

From (7), we know the phase-dependent amplitude variation will cause performance degradation due to the misalignment of the interested signal at the intended receivers. Besides, it is challenging to design the joint active and passive beamforming due to the complicated expression of (7). By considering the phase-dependent amplitude variation, the total transmit power minimization problem was formulated in [106] subject to individual SINR constraints, and it can be solved by the RCO method and the AO method for single-user and multi-user MISO cases, respectively.

4.2.3 *Transmit/receive signal distortion*

There exists transmit/receive signal distortion due to the inevitable hardware impairments of amplifiers, oscillators, DACs, and analog-to-digital converters (ADCs), which results in misalignment of the reflected signal and degrades the transmission performance. In particular, the received signal-to-noise ratio (SNR) maximization problem was studied in [107] by considering transmit/receive signal distortion and it can be solved by using the RCO method and the minorization-maximization algorithm.

4.3 System design under statistical/imperfect CSI

In this part, we consider the system design for the RAWC with statistical CSI or imperfect CSI.

4.3.1 *Statistical CSI*

To avoid the large number of training overhead in the channel estimation, some studies focus on the joint active and passive beamforming design by using statistical CSI [108–110]. Specifically, for an RIS-aided MISO system, the statistical Rician fading CSI was assumed to be available in [108]. In this paper, a tight upper bound of the ergodic capacity was formulated, where the optimal solution of the joint

active and passive beamforming was derived by applying the RCO method. In [109], a model-free based passive beamforming design for the average achievable rate maximization was studied without assuming any specific channel model. Then, this problem was solved by applying stochastic successive convex approximation (SSCA) with the RCO algorithm. For an RIS-aided MIMO system, the work in [110] characterized the spatial correlation of the MIMO channel and applied the AO method to solve the achievable ergodic capacity maximization problem.

4.3.2 *Imperfect CSI*

In practice, the estimated CSI is usually imperfect due to the inherent noise and limited training overhead. This misguides the joint active and passive beamforming design and leads to certain performance degradation. Therefore, it is crucial to investigate the robust beamforming design in RIS-assisted systems. Without loss of generality, we review the following two classical imperfect CSI models, namely the worst-case model and the stochastic model.

Worst-case model. In the worst-case model, the CSI is assumed to be bounded within a certain region. In this model, we usually concern on the system performance with the worst-case channel conditions. For example, the robust joint active and passive beamforming design was studied in [111] for a multi-user MISO system and in [112] for a multi-user MISO CR system. Specifically, the AO method was applied to deal with the coupled active and passive beamformer and S-procedure was proposed to handle the non-convex terms stemming from the channel uncertainty. In addition, the tradeoff between the training overhead and the energy efficiency was investigated in [113] for a single-user MIMO system with a joint robust active and passive beamforming scheme.

Stochastic model. In the stochastic model, the CSI uncertainty is assumed as a random variable with a known prior distribution. For this model, we usually care about the system performance with its outage probability. In [114, 115], the robust joint active and passive beamforming design was studied to minimize total transmission power subject to the individual outage probability constraint, where S-procedure and SSCA were applied to tackle the non-convex terms in the outage probability. Besides, the statistical information such as the distribution of the locations of the users and the distribution of the multi-path channels was considered in [116] for a sum-rate maximization problem. This problem was solved by a two-phase optimization algorithm consisting of the offline phase for the long term and the online phase for the short term.

5 RIS-based information transmission

In RBIT, the RIS acts as an information transmitter that modulates its own messages over the ambient RF radio wave by proactively varying reflection coefficients and then transmits the coded signals to the targeted receiver [22, 23]. Specifically, RBIT is achieved via passive reflection, which is free from power-consuming active components to generate the RF carrier, including oscillators, up-converters, and power amplifiers. Besides, although RIS has limited signal processing ability to achieve high order modulation and complex coding schemes, the large-scale deployment of REs can provide considerable spatial multiplexing or substantial diversity. Motivated by the above potential advantages, in this section, we briefly review the system design of RBIT by considering the ambient RF radio wave with modulated or unmodulated signals.

5.1 RBIT with unmodulated signals

In this part, we mainly investigate the RBIT with the ambient RF radio wave with unmodulated signals. As shown in Figure 6, the RIS-based transmitter attempts to transmit its message w to the RIS receiver by leveraging the RF carrier emitted from the active transmitter. In particular, the active transmitter radiates a monotone RF signal towards RIS. Then, the RIS-based transmitter directly reflects the monotone signal with the amplitude and phase variations according to its transmit symbol, thus achieving the signal modulation in the current RF frequency. RBIT is similar to backscatter communications which usually realize the point-to-point transmission with a single RE. However, the RIS-based transmitter is able to support multi-user transmission simultaneously with the extended transmission range thanks to a large number of REs. To make full potentials of RBIT, it is crucial to design the proper map-

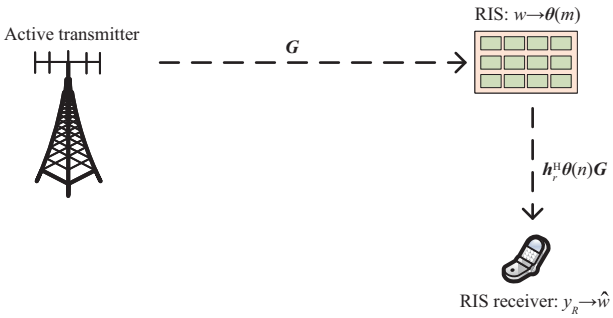

Figure 6 (Color online) RBIT with unmodulated signals: the active transmitter provides the RIS with the unmodulated signals as the RF carrier.

ping between the message symbol and the reflecting pattern, or equivalently modulation scheme, with hardware-constrained REs.

As aforementioned, it is thought that the REs usually vary the phase of the incident signal. Elaborating its phase-shift ability, the RIS-based transmitter can easily achieve the phase shift-keying (PSK) modulation. Specifically, the RIS first optimizes its introduced phases to maximize the received SNR, and then introduces additional phase variations to make the received signal aligned with the same phase shift, creating a virtual bi-dimensional M-ary signal constellation diagram at the receiver [117]. The prototype of RIS-based transmitter with 8×32 REs was proposed in [118] to achieve a high data rate transmission with 8-PSK. Furthermore, the receive antenna indices were exploited in [119] to improve the spectral efficiency with index modulation. In spite of the phase modulation, the RIS-based transmitter could also achieve quadrature amplitude modulation (QAM) with a time-varying reflection coefficient [120]. Later on, the work in [56] investigated the feasibility of using RIS for MIMO transmission with the above QAM scheme, which also showed the great potential to achieve high spectral efficiency with the low-cost RIS-based transmitter.

In addition to supporting a single user with high rate transmission, the RIS-based transmitter is able to serve multiple users at the same time. However, compared with the traditional MIMO transmitter design, it is more challenging to manage the user interference with the unit-modulus constraint. These powerful precoding designs, like zero forcing, maximal ratio transmission, cannot be directly adopted due to the hardware limitation of RIS. To tackle this problem, the authors in [121] considered a multi-user downlink precoding optimization problem and proposed an auto-scaled unit-modulus LS based iterative algorithm. To fully exploit the flexibility of RIS, the RIS-based transmitter adopted constructive symbol-level precoding to turn the harmful multi-user interference into a beneficial signal component [122].

5.2 RBIT with modulated signals

In the remaining part, we further investigate the RBIT with the modulated signal. As shown in Figure 7, the RIS-based transmitter embeds its message w_1 into the modulated signal which is already embedded with the active transmitter message w_2 via the reflection modulation. The receiver aims to decode the message w_1 and probably message w_2 which depends on its decoding strategy. As the active transmitter provides the modulated signal rather than the unmodulated one, the reflected signal is embedded with two messages w_1 and w_2. Moreover, the receiver can also receive the signal from the active transmitter if the link between them is strong enough. Thus, the RIS-based transmission has to tackle the modulated signal smartly, otherwise it will cause additional interference to the receiver, leading to a poor performance. To solve this problem, the collaboration between the RIS-based and active transmissions is needed. In the following, we will show that as the collaboration becomes closer, the relationship between the RIS-based and active transmissions will gradually become mutualistic.

5.2.1 *Interference*

As shown in Figure 4(a), for the worst case, there is no collaboration between the RIS-based and active transmissions. The RIS-based transmitter just exploits the modulated signals as an imperfect carrier signal, and the RIS receiver is designed to recover the message w_1 from the RIS only. Despite the multiple REs, this system is somehow similar to the ambient backscatter communication (AmBC) [123]. Due to lack of collaboration, the two kinds of transmissions will cause interference to each other. Especially for the

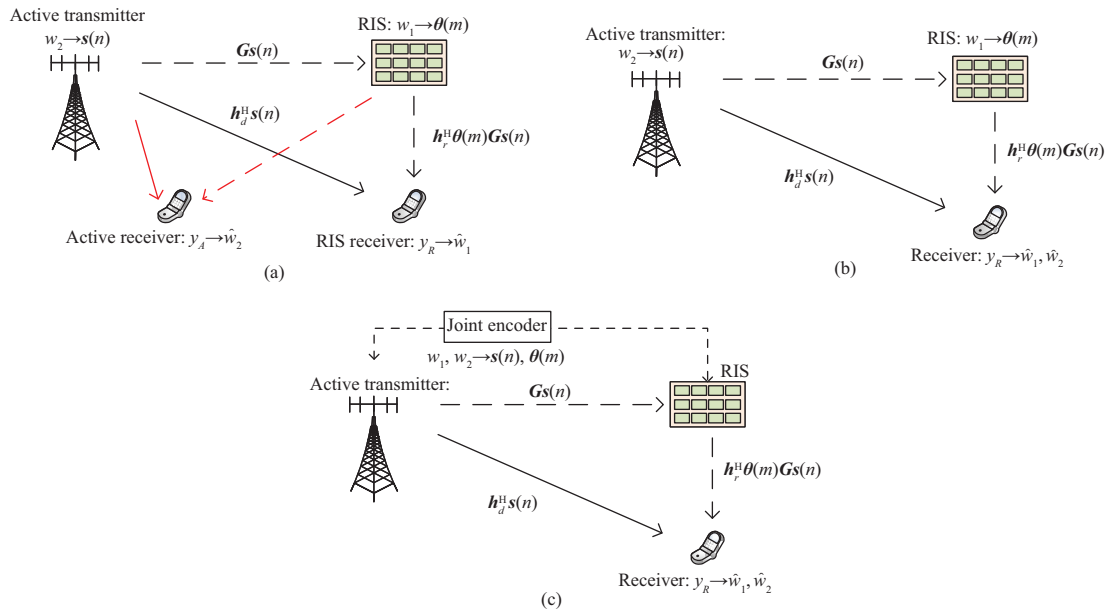

Figure 7 (Color online) RBIT with the modulated signals. (a) Interference. The active transmitter and RIS-based transmitter send information to their individual receivers. The active receiver and RIS receiver only decode their own messages. (b) SR with joint decoding. The active transmitter and RIS-based transmitter send the separated messages to the same receiver. The receiver jointly decodes the messages. (c) SR with joint encoding and decoding. The active transmitter and RIS-based transmitter send the joint messages generated by the joint encoder to the receiver. The receiver jointly decodes the messages.

RIS transmission, its performance may suffer severe direct-link interference from the active transmitter. Moreover, as the receiver has no knowledge of the symbols from the active transmitter, the RIS receiver generally adopts noncoherent detection, which has lower performance compared to coherent detection.

As for the direct-link interference problem, some literatures in AmBC proposed a frequency-shifting method to avoid the direct-link interference [124, 125], and others exploited the waveform feature to cancel out the interference [24, 126]. To tackle the imperfect carrier signal, the authors in [127] exploited the large degree of freedoms in RIS to let a slave antenna only receive the direct-link signal, and thus by normalizing the signals at the other antenna, the receiver can cancel the unknown source symbols. This work achieves multi-user downlink RIS-based transmission with the commodity Wi-Fi signals. Nevertheless, the modulated carrier signal is still not so ideal that the RIS-based transmission without any collaboration undergoes unsatisfactory achievement.

5.2.2 *Symbiotic radio*

Such mutual interference in the above subsection can be avoided via forming the SR between the RIS-based transmission and the active transmission [29, 30, 128], as the SR encourages these two kinds of transmission to collaborate with each other and achieve the mutualistic benefits together. Specifically, in SR, the active transmission system shares the spectrum and energy with the RIS-based transmission and enables the RIS to perform the reflection pattern modulation via reflecting the existing active signal. In addition, the RIS receiver is designed to have the prior knowledge on the codebooks of the two transmissions and is thus able to adopt the joint decoding to decode the message w_1 and w_2 at the same time. As the receiver decodes the message w_2 from the active transmitter, the direct-link interference can be directly canceled, and also the RIS symbol detection processing is therefore coherent. In return, the RIS also provides the multipath diversity to the active transmission via the opportunistic reflection, thereby enhancing the active transmission.

As a newly emerging communication paradigm, the SR was first introduced in [128], and the joint decoding strategy based on maximum likelihood detection was first proposed in [129] with a single RE. However, the SR with a single RE suffers from the additional path-loss introduced by the reflection and thus has poor performance. Therefore, the RIS with a large number of REs can be exploited to improve the performance of the SR. An RIS-based SR was proposed in [30], which showed that the RIS-based SR can reduce the overall power consumption with more REs deployed at the RIS. Besides, RIS-based SR can realize more sophisticated reflection modulation schemes to support more users [130]. Spatial

modulation was elaborated at the RIS to improve the transmission rate of the SR system [119].

The RIS-based transmitter and the active transmitter in the above design encode their messages w_1 and w_2 separately. However, the active transmitter can collaborate with the RIS via a joint encoder and the joint encoding strategy can be exploited to encode messages w_1 and w_2 together, which is shown in Figure 4(c). The joint encoding is naturally superior to the separate encoding, since the separate encoding is actually a special case of the joint encoding. Moreover, with the collaboration between the active and RIS-based transmissions going closer, the system has better overall BER and rate performances than other aforementioned schemes, which were validated via the simulation results in [131, 132], respectively. Although these collaborations usually come at the expense of additional hardware costs and computational complexity, it provides a promising way ahead to SR, which changes the interfering spectrum sharing into mutually beneficial spectrum sharing.

6 Potential applications in 6G networks

As aforementioned, 6G is expected to fulfill more stringent requirements on transmission capacity, reliability, latency, coverage, energy consumption, and connection density [2, 3]. Specifically, 6G should support the following typical usage scenarios: (1) Ultra-massive machine-type communications (umMTC): the device connectivity density is larger than 10^7 devices/km^2 [2]; (2) Extremely reliable and low-latency communications (ERLLC): the reliability should be higher than 99.9999% and the latency should be smaller than 100 μs [133]; (3) Further-enhanced mobile broadband (FeMBB): the peak data rate should be at least 1 Tb/s and the user-experienced data rate should be higher than 1 Gb/s [2]; (4) Extremely low-power communications (ELPC): the energy efficiency should be ten or hundred times of 5G.

To fulfill these typical stringent requirements, various promising technologies, such as Terahertz (THz) communications, short packet communications (SPC), visible light communications (VLC), and mobile edge computing (MEC), have been proposed. Moreover, RIS can be jointly designed with these technologies and brings additional degrees of freedom to meet the stringent requirements of 6G. This is because the RIS has the capability of building a controllable and programmable wireless environment without additional energy consumption. In the following, we will show some potential applications of RIS in 6G networks.

6.1 Massive connectivity communications

With the rise of Internet-of-Things (IoT), umMTC will be an important usage scenario of 6G networks. However, a large number of IoT devices are usually located in a dead-zone where the transmitted signals, especially for high-frequency signals, suffer from deep fading. One solution to this problem is deploying RIS into umMTC systems since it can enhance the signal transmission by passive beamforming. Specifically, the work in [134] exploited the sum mean squared error criterion to design the active and passive beamformers jointly for an RIS-aided massive access system. However, the above joint beamforming design requires the CSI and the channel estimation for such a system needs a larger training overhead than conventional massive connectivity systems because the passive RIS cannot perform active transmitting/receiving. In [135], the sporadic traffic pattern of machine-type communications was considered for an RIS-aided massive access MISO system, where a matrix factorization based SCCE method was proposed to perform the joint user activity detection and channel estimation. Moreover, to further reduce the training overhead, how to make use of channel distribution, channel sparsity, and common channel knowledge, to reduce the training overhead for RIS-aided massive connectivity systems is an interesting topic in the future.

6.2 THz communications

THz communications operating between 100 GHz and 10 THz is considered as a key enabler for FeMBB in 6G due to the extremely large bandwidth. However, high-frequency signals are much likely blocked due to high penetration loss and reduced diffraction effects. Hence, RIS can be deployed in THz communications to alleviate the severe propagation attenuation. Specifically, the joint hybrid precoding strategy was considered in [136] to maximize the sum-rate for RIS-aided THz MIMO communication systems. Then, in the same system of [136], the hierarchical search codebook design was proposed in [137] to achieve a low-complexity basis of beam training for channel estimation and data transmission. In [138], the

RIS was mounted on a satellite to enable signal propagation in low earth orbit satellite networks with THz communications, where the theoretical error rate expressions caused by the misalignment fading were analyzed. Besides, in [139], the joint optimization of unmanned aerial vehicle trajectory, active and passive beamforming, power, and THz sub-band allocation was studied to maximize the minimum average achievable rate of all users. Inspired by these studies, how to deploy the RIS by jointly considering the RIS location, path-loss, active and passive beamforming, and other system characteristics for performance enhancement is an interesting field to be studied.

6.3 Short packet communications

SPC is one of the prominent solutions to achieve ERLLC in 6G. However, the system design with SPC in the RIS-assisted system is quite different from that in conventional systems due to double fading cascaded channel and hardware impairments of RIS. In [140], the average achievable rate and error probability were investigated for an RIS-aided system with a finite blocklength regime, and the impacts of phase error caused by the limited quantization levels or hardware impairments on the rate and error probability were further analyzed. Besides, it is also necessary to reconsider the joint optimization of user transmission scheduling, data packet length, and active and passive beamforming for the RIS-aided systems with SPC to improve the target transmission rate and the reliability, and to reduce the transmission latency.

6.4 Visible light communications

VLC is a promising technology to meet the capacity demands of 6G since it can enable the information exchange over the unlicensed visible spectrum. However, the full potential performance of VLC is limited by the transmission distance, usually between 2–5 m. Thus, the RIS can be introduced into VLC to mitigate intensity loss and enhance signal transmission of VLC. Specifically, the reflection pattern design of RIS was investigated in [141] to extend the communication range. In addition, the RIS-assisted dual-hop VLC system was studied in [142], where the optical signal was first converted into the RF signal by a relay and then transmitted to the intended receiver through RIS. Then, the outage probability and bit error rate were further derived based on the above model. Therefore, how to jointly design the RIS active and passive beamformers to enhance the VLC is an interesting problem to be solved.

6.5 Mobile edge computing

MEC is a promising technology to support low-latency services with high-performance because it can enable the resource-limited devices to partially offload their computation tasks to the nearby computing nodes. However, the potential benefits of MEC systems are limited due to the long-distance offloading link. This problem can be resolved by deploying an RIS to enhance the signal transmission by passive beamforming. Specifically, the RIS-assisted MEC systems were considered in [143], which provides solutions to various objectives including shortening processing latency, improving energy efficiency, and enhancing total completed task-input bit. Then, the total completed task-input bits of all users in an RIS-assisted MEC systems was considered in [144] subject to energy budgets. Therefore, it is a crucial problem to jointly design the active and passive beamformers, RIS deployment, communications, and computing resource allocation of RIS-aided MEC systems to further enhance the uplink offloading performance and system performance. Moreover, since MEC can provide rich computation resources for artificial intelligence based networks, how to jointly design the RIS with various objectives in the mobile edge learning system to achieve higher system performance is also an interesting problem.

6.6 Air-ground communications

A large dimensional air-ground network is expected in 6G due to the expanded requirements of data transmission for aerial users. However, the channels between terrestrial users and aerial users are usually strong line-of-sight links due to the open space, which introduces high inter-cell interference and degrades the transmission performance. In order to mitigate inter-cell interference and improve the network capacity, the RIS was deployed into the air-ground communications with multiple aerial/terrestrial users [145], in which the RIS placement and the active and passive beamformers are jointly designed. Besides, in [146], the aerial user trajectory was further considered in the above system to achieve a higher spectrum and energy efficiency. Hence, how to jointly optimize the RIS deployment and the active and

passive beamformers for interference cancellation and transmission enhancement is an impotent problem to be solved.

6.7 Network security

The strict privacy and security should be supported due to the ubiquitous and unlimited wireless connectivity in the large dimensional integrated system of 6G. Specifically, in the physical layer, RIS can provide the secure communication systems with additional communication links so as to enhance the transmission of the legitimate receivers while suppressing the transmission of the eavesdroppers [88–91]. Furthermore, the artificial noise was further considered in [92] to improve the capacity of secure communication. Besides, it is crucial to jointly design the RIS passive beamformer with other secure technologies, e.g., secure channel coding, quantum communications and computing, and deep learning algorithms to predict potential attacks and improve data privacy and communication security.

7 Conclusion

This paper has provided an overview of the fundamental physical layer issues of the RIS-assisted wireless systems, including reflection principle and channel estimation, and system designs for RAWC and RBIT. Specifically, we have summarized the main state-of-the-art solutions to each problem and briefly stated the advantages/disadvantages of these solutions. Moreover, we have envisioned the related potential applications of RIS in the 6G networks. As an emerging spectrum-/energy-/cost-efficient technique, there are still many open issues and challenges when deploying RIS into reality. We hope that this paper can be a useful handbook for researchers to find benchmark schemes and effective guidance for future research in 6G networks.

Acknowledgements This work was supported in part by National Natural Science Foundation of China (Grant Nos. U1801261, 61631005), in part by National Key R&D Program of China (Grant No. 2018YFB1801105), in part by Macau Science and Technology Development Fund (FDCT), Macau SAR (Grant No. 0009/2020/A1), in part by Key Areas of Research and Development Program of Guangdong Province (Grant No. 2018B010114001), in part by Programme of Introducing Talents of Discipline to Universities (Grant No. B20064), and in part by Fundamental Research Funds for the Central Universities (Grant No. ZYGX2019Z022).

References

1 You X H, Wang C X, Huang J, et al. Towards 6G wireless communication networks: vision, enabling technologies, and new paradigm shifts. Sci China Inf Sci, 2021, 64: 110301
2 Zhang Z Q, Xiao Y, Ma Z, et al. 6G wireless networks: vision, requirements, architecture, and key technologies. IEEE Veh Technol Mag, 2019, 14: 28–41
3 Zhang L, Liang Y C, Niyato D. 6G visions: mobile ultra-broadband, super Internet-of-Things, and artificial intelligence. China Commun, 2019, 16: 1–14
4 Liang Y C. Dynamic Spectrum Management: from Cognitive Radio to Blockchain and Artificial Intelligence. Berlin: Springer, 2020
5 Liang Y C, Long R Z, Zhang Q Q, et al. Large intelligent surface/antennas (LISA): making reflective radios smart. J Commun Inf Netw, 2019, 4: 40–50
6 Dai L L, Wang B C, Wang M, et al. Reconfigurable intelligent surface-based wireless communications: antenna design, prototyping, and experimental results. IEEE Access, 2020, 8: 45913–45923
7 Wu Q Q, Zhang R. Towards smart and reconfigurable environment: intelligent reflecting surface aided wireless network. IEEE Commun Mag, 2020, 58: 106–112
8 Gong S, Lu X, Hoang D T, et al. Toward smart wireless communications via intelligent reflecting surfaces: a contemporary survey. IEEE Commun Surv Tut, 2020, 22: 2283–2314
9 Wu Q Q, Zhang S W, Zheng B X, et al. Intelligent reflecting surface aided wireless communications: a tutorial. IEEE Trans Commun, 2021. doi: 10.1109/TCOMM.2021.3051897
10 Yuan X J, Zhang Y J A, Shi Y M, et al. Reconfigurable-intelligent-surface empowered wireless communications: challenges and opportunities. IEEE Wirel Commun, 2021. doi: 0.1109/MWC.001.2000256
11 Renzo M D, Debbah M, Phan-Huy D T, et al. Smart radio environments empowered by reconfigurable AI meta-surfaces: an idea whose time has come. J Wirel Com Netw, 2019, 2019: 129
12 di Renzo M, Zappone A, Debbah M, et al. Smart radio environments empowered by reconfigurable intelligent surfaces: how it works, state of research, and the road ahead. IEEE J Sel Areas Commun, 2020, 38: 2450–2525
13 Huang C W, Hu S, Alexandropoulos G C, et al. Holographic MIMO surfaces for 6G wireless networks: opportunities, challenges, and trends. IEEE Wirel Commun, 2020, 27: 118–125
14 di Renzo M, Ntontin K, Song J, et al. Reconfigurable intelligent surfaces vs. relaying: differences, similarities, and performance comparison. IEEE Open J Commun Soc, 2020, 1: 798–807
15 Liu Y W, Liu X, Mu X D, et al. Reconfigurable intelligent surfaces: principles and opportunities. 2020. ArXiv:2007.03435
16 Tang W, Chen M Z, Chen X, et al. Wireless communications with reconfigurable intelligent surface: path loss modeling and experimental measurement. IEEE Trans Wirel Commun, 2021, 20: 421–439
17 Tang W K, Chen X Y, Chen M Z, et al. Path loss modeling and measurements for reconfigurable intelligent surfaces in the millimeter-wave frequency band. 2021. ArXiv:2101.08607

18 Gacanin H, di Renzo M. Wireless 2.0: toward an intelligent radio environment empowered by reconfigurable meta-surfaces and artificial intelligence. IEEE Veh Technol Mag, 2020, 15: 74–82
19 Elbir A M, Mishra K V. A survey of deep learning architectures for intelligent reflecting surfaces. 2020. ArXiv:2009.02540
20 Gao F F, Cui T, Nallanathan A. On channel estimation and optimal training design for amplify and forward relay networks. IEEE Trans Wirel Commun, 2008, 7: 1907–1916
21 Yang S, Belfiore J C. Towards the optimal amplify-and-forward cooperative diversity scheme. IEEE Trans Inform Theor, 2007, 53: 3114–3126
22 Li Q, Wen M W, Di Renzo M. Single-RF MIMO: from spatial modulation to metasurface-based modulation. 2020. ArXiv:2009.00789
23 Lin S E, Zheng B X, Alexandropoulos G C, et al. Reconfigurable intelligent surfaces with reflection pattern modulation: beamforming design and performance analysis. IEEE Trans Wirel Commun, 2020, 20: 741–754
24 Yang G, Liang Y C, Zhang R, et al. Modulation in the air: backscatter communication over ambient OFDM carrier. IEEE Trans Commun, 2018, 66: 1219–1233
25 Yang G, Ho C K, Guan Y L. Multi-antenna wireless energy transfer for backscatter communication systems. IEEE J Sel Areas Commun, 2015, 33: 2974–2987
26 Kang X, Liang Y C, Yang J. Riding on the primary: a new spectrum sharing paradigm for wireless-powered IoT devices. IEEE Trans Wirel Commun, 2018, 17: 6335–6347
27 Liu W, Liang Y C, Li Y, et al. Backscatter multiplicative multiple-access systems: fundamental limits and practical design. IEEE Trans Wirel Commun, 2018, 17: 5713–5728
28 Fara R, Phan-Huy D T, Ratajczak P, et al. Reconfigurable intelligent surface-assisted ambient backscatter communications — experimental assessment. 2021. ArXiv:2103.08427
29 Liang Y C, Zhang Q, Larsson E G, et al. Symbiotic radio: cognitive backscattering communications for future wireless networks. IEEE Trans Cogn Commun Netw, 2020, 6: 1242–1255
30 Zhang Q, Liang Y C, Poor H V. Large intelligent surface/antennas (LISA) assisted symbiotic radio for IoT communications. 2020. ArXiv:2002.00340
31 Gradoni G, di Renzo M. End-to-end mutual coupling aware communication model for reconfigurable intelligent surfaces: an electromagnetic-compliant approach based on mutual impedances. IEEE Wirel Commun Lett, 2021, 10: 938–942
32 Qian X W, di Renzo M. Mutual coupling and unit cell aware optimization for reconfigurable intelligent surfaces. IEEE Wirel Commun Lett, 2021. doi: 10.1109/LWC.2021.3061449
33 Abrardo A, Dardari D, Di Renzo M, et al. MIMO interference channels assisted by reconfigurable intelligent surfaces: mutual coupling aware sum-rate optimization based on a mutual impedance channel model. 2021. ArXiv:2102.07155
34 Abeywickrama S, Zhang R, Wu Q Q, et al. Intelligent reflecting surface: practical phase shift model and beamforming optimization. IEEE Trans Commun, 2020, 68: 5849–5863
35 Wang D, Yin L Z, Huang T J, et al. Design of a 1 bit broadband space-time-coding digital metasurface element. Anten Wirel Propag Lett, 2020, 19: 611–615
36 Huang C, Sun B, Pan W B, et al. Dynamical beam manipulation based on 2-bit digitally-controlled coding metasurface. Sci Rep, 2017, 7: 42302
37 Xu H J, Xu S H, Yang F, et al. Design and experiment of a dual-band 1 bit reconfigurable reflectarray antenna with independent large-angle beam scanning capability. Anten Wirel Propag Lett, 2020, 19: 1896–1900
38 Yang H H, Yang F, Xu S H, et al. A 1-bit multipolarization reflectarray element for reconfigurable large-aperture antennas. Anten Wirel Propag Lett, 2017, 16: 581–584
39 Wang Z L, Ge Y H, Pu J X, et al. 1 bit electronically reconfigurable folded reflectarray antenna based on p-i-n diodes for wide-angle beam-scanning applications. IEEE Trans Anten Propag, 2020, 68: 6806–6810
40 Yang H H, Yang F, Xu S H, et al. A 1-Bit 10×10 reconfigurable reflectarray antenna: design, optimization, and experiment. IEEE Trans Anten Propag, 2016, 64: 2246–2254
41 Han J, Li L, Liu G, et al. A wideband 1 bit 12×12 reconfigurable beam-scanning reflectarray: design, fabrication, and measurement. Anten Wirel Propag Lett, 2019, 18: 1268–1272
42 Li Y Z, Abbosh A. Reconfigurable reflectarray antenna using single-layer radiator controlled by PIN diodes. IET Microw Anten Propag, 2015, 9: 664–671
43 Yang H H, Yang F, Cao X Y, et al. A 1600-element dual-frequency electronically reconfigurable reflectarray at X/Ku-band. IEEE Trans Anten Propag, 2017, 65: 3024–3032
44 Yang X, Xu S H, Yang F, et al. A novel 2-bit reconfigurable reflectarray element for both linear and circular polarizations. In: Proceedings of IEEE International Symposium on Antennas and Propagation and USNC/URSI National Radio Science Meeting, 2017. 2083–2084
45 Venneri F, Costanzo S, di Massa G. Design and validation of a reconfigurable single varactor-tuned reflectarray. IEEE Trans Anten Propag, 2013, 61: 635–645
46 Ratni B, de Lustrac A, Piau G P, et al. Active metasurface for reconfigurable reflectors. Appl Phys A, 2018, 124: 104
47 Trampler M E, Lovato R E, Gong X. Dual-resonance continuously beam-scanning x-band reflectarray antenna. IEEE Trans Anten Propag, 2020, 68: 6080–6087
48 Yang X, Xu S H, Yang F, et al. Design of a 2-bit reconfigurable reflectarray element using two MEMS switches. In: Proceedings of IEEE International Symposium on Antennas and Propagation and USNC/URSI National Radio Science Meeting, 2015. 2167–2168
49 Debogovic T, Perruisseau-Carrier J. Low loss MEMS-reconfigurable 1-bit reflectarray cell with dual-linear polarization. IEEE Trans Anten Propag, 2014, 62: 5055–5060
50 Bayraktar O, Civi O A, Akin T. Beam switching reflectarray monolithically integrated with RF MEMS switches. IEEE Trans Anten Propag, 2012, 60: 854–862
51 Yang J, Wang P J, Sun S Y, et al. A novel electronically controlled two-dimensional terahertz beam- scanning reflectarray antenna based on liquid crystals. Front Phys, 2020, 8: 435
52 Perez-Palomino G, Baine P, Dickie R, et al. Design and experimental validation of liquid crystal-based reconfigurable reflectarray elements with improved bandwidth in F-band. IEEE Trans Anten Propag, 2013, 61: 1704–1713
53 Carrasco E, Perruisseau-Carrier J. Reflectarray antenna at terahertz using graphene. Anten Wirel Propag Lett, 2013, 12: 253–256
54 Hamzavi-Zarghani Z, Yahaghi A, Matekovits L. Reconfigurable metasurface lens based on graphene split ring resonators using Pancharatnam-Berry phase manipulation. J ElectroMagn Waves Appl, 2019, 33: 572–583

55 Dong L, Wang H M. Enhancing secure MIMO transmission via intelligent reflecting surface. IEEE Trans Wirel Commun, 2020, 19: 7543–7556
56 Tang W, Dai J Y, Chen M Z, et al. MIMO transmission through reconfigurable intelligent surface: system design, analysis, and implementation. IEEE J Sel Areas Commun, 2020, 38: 2683–2699
57 Zhang L, Wang Z X, Shao R W, et al. Dynamically realizing arbitrary multi-bit programmable phases using a 2-bit time-domain coding metasurface. IEEE Trans Anten Propag, 2020, 68: 2984–2992
58 Li L L, Shuang Y, Ma Q, et al. Intelligent metasurface imager and recognizer. Light Sci Appl, 2019, 8: 97
59 Pan X T, Yang F, Xu S H, et al. A 10 240-element reconfigurable reflectarray with fast steerable monopulse patterns. IEEE Trans Anten Propag, 2021, 69: 173–181
60 Huang J. Microstrip reflectarray. In: Proceedings of Antennas and Propagation Society Symposium 1991 Digest, 1991. 612–615
61 Berry D, Malech R, Kennedy W. The reflectarray antenna. IEEE Trans Anten Propag, 1963, 11: 645–651
62 Chen J, Liang Y C, Pei Y Y, et al. Intelligent reflecting surface: a programmable wireless environment for physical layer security. IEEE Access, 2019, 7: 82599–82612
63 Wu Q Q, Zhang R. Intelligent reflecting surface enhanced wireless network via joint active and passive beamforming. IEEE Trans Wirel Commun, 2019, 18: 5394–5409
64 Taha A, Alrabeiah M, Alkhateeb A. Enabling large intelligent surfaces with compressive sensing and deep learning. IEEE Access, 2021, 9: 44304–44321
65 Zhang J M, Qi C H, Li P, et al. Channel estimation for reconfigurable intelligent surface aided massive MIMO system. In: Proceedings of the 21st International Workshop on Signal Processing Advances in Wireless Communications (SPAWC), 2020. 1–5
66 He Z Q, Yuan X. Cascaded channel estimation for large intelligent metasurface assisted massive MIMO. IEEE Wirel Commun Lett, 2020, 9: 210–214
67 Liu H, Yuan X J, Zhang Y J A. Matrix-calibration-based cascaded channel estimation for reconfigurable intelligent surface assisted multiuser MIMO. IEEE J Sel Areas Commun, 2020, 38: 2621–2636
68 Guan X R, Wu Q Q, Zhang R. Anchor-assisted intelligent reflecting surface channel estimation for multiuser communications. 2020. ArXiv:2008.00622
69 Wei L, Huang C W, Alexandropoulos G C, et al. Channel estimation for RIS-empowered multi-user MISO wireless communications. IEEE Trans Commun, 2021. doi: 10.1109/TCOMM.2021.3063236
70 de Araújo G T, de Almeida A L. Parafac-based channel estimation for intelligent reflective surface assisted MIMO system. In: Proceedings of the 11st Sensor Array and Multichannel Signal Processing Workshop (SAM), 2020. 1–5
71 Mishra D, Johansson H. Channel estimation and low-complexity beamforming design for passive intelligent surface assisted MISO wireless energy transfer. In: Proceedings of International Conference on Acoustics, Speech and Signal Processing (ICASSP), 2019. 4659–4663
72 Yang Y F, Zheng B X, Zhang S W, et al. Intelligent reflecting surface meets OFDM: protocol design and rate maximization. IEEE Trans Commun, 2020, 68: 4522–4535
73 Jensen T L, de Carvalho E. An optimal channel estimation scheme for intelligent reflecting surfaces based on a minimum variance unbiased estimator. In: Proceedings of IEEE International Conference on Acoustics, Speech and Signal Processing (ICASSP), 2020. 5000–5004
74 Sun S, Yan H S. Channel estimation for reconfigurable intelligent surface-assisted wireless communications considering doppler effect. IEEE Wirel Commun Lett, 2021, 10: 790–794
75 Zheng B X, Zhang R. Intelligent reflecting surface-enhanced OFDM: channel estimation and reflection optimization. IEEE Wirel Commun Lett, 2020, 9: 518–522
76 Kundu N K, McKay M R. A deep learning-based channel estimation approach for MISO communications with large intelligent surfaces. In: Proceedings of the 31st Annual International Symposium on Personal, Indoor and Mobile Radio Communications, 2020. 1–6
77 Liu C, Liu X M, Ng D W K, et al. Deep residual network empowered channel estimation for IRS-assisted multi-user communication systems. 2020. ArXiv:2012.00241
78 Wang Z R, Liu L, Cui S G. Channel estimation for intelligent reflecting surface assisted multiuser communications: framework, algorithms, and analysis. IEEE Trans Wirel Commun, 2020, 19: 6607–6620
79 Zheng B X, You C S, Zhang R. Intelligent reflecting surface assisted multi-user OFDMA: channel estimation and training design. IEEE Trans Wirel Commun, 2020, 19: 8315–8329
80 Chen J, Liang Y C, Cheng H V, et al. Channel estimation for reconfigurable intelligent surface aided multi-user MIMO systems. 2019. ArXiv:1912.03619
81 Nadeem Q U A, Kammoun A, Chaaban A, et al. Asymptotic max-min SINR analysis of reconfigurable intelligent surface assisted MISO systems. IEEE Trans Wirel Commun, 2020, 19: 7748–7764
82 Guo H, Liang Y C, Chen J, et al. Weighted sum-rate maximization for reconfigurable intelligent surface aided wireless networks. IEEE Trans Wirel Commun, 2020, 19: 3064–3076
83 Huang C, Zappone A, Alexandropoulos G C, et al. Reconfigurable intelligent surfaces for energy efficiency in wireless communication. IEEE Trans Wirel Commun, 2019, 18: 4157–4170
84 Yang G, Xu X Y, Liang Y C. Intelligent reflecting surface assisted non-orthogonal multiple access. In: Proceedings of IEEE Wireless Communications and Networking Conference (WCNC), 2020. 1–6
85 Mu X D, Liu Y W, Guo L, et al. Exploiting intelligent reflecting surfaces in NOMA networks: joint beamforming optimization. IEEE Trans Wirel Commun, 2020, 19: 6884–6898
86 Zhang L, Wang Y, Tao W G, et al. Intelligent reflecting surface aided MIMO cognitive radio systems. IEEE Trans Veh Technol, 2020, 69: 11445–11457
87 Cui M, Zhang G C, Zhang R. Secure wireless communication via intelligent reflecting surface. IEEE Wirel Commun Lett, 2019, 8: 1410–1414
88 Yu X H, Xu D F, Sun Y, et al. Robust and secure wireless communications via intelligent reflecting surfaces. IEEE J Sel Areas Commun, 2020, 38: 2637–2652
89 Shen H, Xu W, Gong S L, et al. Secrecy rate maximization for intelligent reflecting surface assisted multi-antenna communications. IEEE Commun Lett, 2019, 23: 1488–1492
90 Hu S K, Wei Z Q, Cai Y X, et al. Robust and secure sum-rate maximization for multiuser MISO downlink systems with self-sustainable IRS. 2021. ArXiv:2101.10549

91 Chu Z, Hao W M, Xiao P, et al. Intelligent reflecting surface aided multi-antenna secure transmission. IEEE Wireless Commun Lett, 2020, 9: 108–112
92 Hong S, Pan C H, Ren H, et al. Artificial-noise-aided secure MIMO wireless communications via intelligent reflecting surface. IEEE Trans Commun, 2020, 68: 7851–7866
93 Long R, Liang Y C, Pei Y, et al. Active reconfigurable intelligent surface aided wireless communications. IEEE Trans Wirel Commun, 2021. doi: 10.1109/TWC.2021.3064024
94 Lyu B, Hoang D T, Gong S M, et al. Intelligent reflecting surface assisted wireless powered communication networks. In: Proceedings of IEEE Wireless Communications and Networking Conference Workshops (WCNCW), 2020. 1–6
95 Wu Q Q, Zhang R. Joint active and passive beamforming optimization for intelligent reflecting surface assisted SWIPT under QoS constraints. IEEE J Sel Areas Commun, 2020, 38: 1735–1748
96 Perović N S, Tran L N, Di Renzo M, et al. Achievable rate optimization for MIMO systems with reconfigurable intelligent surfaces. IEEE Trans Wirel Commun, 2021. doi: 10.1109/TWC.2021.3054121
97 Perović N S, Tran L N, Di Renzo M, et al. Optimization of RIS-aided MIMO systems via the cutoff rate. 2020. ArXiv:2012.05131
98 Huang C, Mo R, Yuen C. Reconfigurable intelligent surface assisted multiuser MISO systems exploiting deep reinforcement learning. IEEE J Sel Areas Commun, 2020, 38: 1839–1850
99 Yang H L, Xiong Z H, Zhao J, et al. Deep reinforcement learning-based intelligent reflecting surface for secure wireless communications. IEEE Trans Wirel Commun, 2021, 20: 375–388
100 Lee G, Jung M, Kasgari A T Z, et al. Deep reinforcement learning for energy-efficient networking with reconfigurable intelligent surfaces. In: Proceedings of IEEE International Conference on Communications (ICC), 2020. 1–6
101 Huang C W, Yang Z H, Alexandropoulos G C, et al. Multi-hop RIS-empowered terahertz communications: a DRL-based hybrid beamforming design. IEEE J Sel Areas Commun, 2021. doi: 10.1109/JSAC.2021.3071836
102 Li D. Ergodic capacity of intelligent reflecting surface-assisted communication systems with phase errors. IEEE Commun Lett, 2020, 24: 1646–1650
103 Wu Q Q, Zhang R. Beamforming optimization for wireless network aided by intelligent reflecting surface with discrete phase shifts. IEEE Trans Commun, 2020, 68: 1838–1851
104 Zhao M M, Wu Q Q, Zhao M J, et al. IRS-aided wireless communication with imperfect CSI: is amplitude control helpful or not? In: Proceedings of IEEE Global Communications Conference, 2020. 1–6
105 Rajagopalan H, Rahmat-Samii Y. Loss quantification for microstrip reflectarray: issue of high fields and currents. In: Proceedings of IEEE Antennas and Propagation Society International Symposium, 2008. 1–4
106 Jung M, Saad W, Debbah M, et al. On the optimality of reconfigurable intelligent surfaces (RISs): passive beamforming, modulation, and resource allocation. IEEE Trans Wirel Commun, 2021. doi: 10.1109/TWC.2021.3058366
107 Shen H, Xu W, Gong S L, et al. Beamforming optimization for IRS-aided communications with transceiver hardware impairments. IEEE Trans Commun, 2021, 69: 1214–1227
108 Han Y, Tang W K, Jin S, et al. Large intelligent surface-assisted wireless communication exploiting statistical CSI. IEEE Trans Veh Technol, 2019, 68: 8238–8242
109 Guo H, Liang Y C, Xiao S. Model-free optimization for reconfigurable intelligent surface with statistical CSI. 2019. ArXiv:1912.10913
110 Zhang J, Liu J, Ma S D, et al. Transmitter design for large intelligent surface-assisted MIMO wireless communication with statistical CSI. In: Proceedings of IEEE International Conference on Communications Workshops, 2020. 1–5
111 Zhou G, Pan C H, Ren H, et al. Robust beamforming design for intelligent reflecting surface aided MISO communication systems. IEEE Wirel Commun Lett, 2020, 9: 1658–1662
112 Yuan J, Liang Y C, Joung J G, et al. Intelligent reflecting surface (IRS)-enhanced cognitive radio system. In: Proceedings of IEEE International Conference on Communications, 2020. 1–6
113 Zappone A, di Renzo M, Shams F, et al. Overhead-aware design of reconfigurable intelligent surfaces in smart radio environments. IEEE Trans Wirel Commun, 2021, 20: 126–141
114 Wang J, Liang Y C, Han S Y, et al. Robust beamforming and phase shift design for IRS-enhanced multi-user MISO downlink communication. In: Proceedings of IEEE International Conference on Communications, 2020. 1–6
115 Zhao M M, Liu A, Zhang R. Outage-constrained robust beamforming for intelligent reflecting surface aided wireless communication. IEEE Trans Signal Process, 2021, 69: 1301–1316
116 Abrardo A, Dardari D, Di Renzo M. Intelligent reflecting surfaces: sum-rate optimization based on statistical CSI. 2020. ArXiv:2012.10679
117 Basar E, di Renzo M, de Rosny J, et al. Wireless communications through reconfigurable intelligent surfaces. IEEE Access, 2019, 7: 116753
118 Tang W, Dai J Y, Chen M, et al. Programmable metasurface-based RF chain-free 8PSK wireless transmitter. Electron lett, 2019, 55: 417–420
119 Basar E. Reconfigurable intelligent surface-based index modulation: a new beyond MIMO paradigm for 6G. IEEE Trans Commun, 2020, 68: 3187–3196
120 Dai J Y, Tang W, Yang L X, et al. Realization of multi-modulation schemes for wireless communication by time-domain digital coding metasurface. IEEE Trans Anten Propag, 2020, 68: 1618–1627
121 Bereyhi A, Jamali V, Muller R R, et al. A single-RF architecture for multiuser massive MIMO via reflecting surfaces. In: Proceedings of IEEE International Conference on Acoustics, Speech and Signal Processing, 2020. 8688–8692
122 Liu R, Li H Y, Li M, et al. Symbol-level precoding design for intelligent reflecting surface assisted multi-user MIMO systems. In: Proceedings of the 11th International Conference on Wireless Communications and Signal Processing, 2019. 1–6
123 Liu V, Parks A, Talla V, et al. Ambient backscatter: wireless communication out of thin air. In: Proceedings of ACM SIGCOMM Conference, 2013. 39–50
124 Iyer V, Talla V, Kellogg B, et al. Inter-technology backscatter: towards internet connectivity for implanted devices. In: Proceedings of ACM SIGCOMM Conference, 2016. 356–369
125 Zhang P Y, Rostami M, Hu P, et al. Enabling practical backscatter communication for on-body sensors. In: Proceedings of ACM SIGCOMM Conference, 2016. 370–383
126 Nguyen T, Shin Y, Kim J, et al. Signal detection for ambient backscatter communication with OFDM carriers. Sensors, 2019, 19: 517
127 Zhao H T, Shuang Y, Wei M L, et al. Metasurface-assisted massive backscatter wireless communication with commodity wi-fi signals. Nat Commun, 2020, 11: 1–10

128 Long R Z, Liang Y C, Guo H Y, et al. Symbiotic radio: a new communication paradigm for passive Internet of Things. IEEE Int Things J, 2020, 7: 1350–1363

129 Yang G, Zhang Q Q, Liang Y C. Cooperative ambient backscatter communications for green Internet-of-Things. IEEE Int Things J, 2018, 5: 1116–1130

130 Yan W J, Yuan X J, He Z Q, et al. Passive beamforming and information transfer design for reconfigurable intelligent surfaces aided multiuser MIMO systems. IEEE J Sel Areas Commun, 2020, 38: 1793–1808

131 Guo S S, Lv S H, Zhang H X, et al. Reflecting modulation. IEEE J Sel Areas Commun, 2020, 38: 2548–2561

132 Karasik R, Simeone O, Di Renzo M, et al. Single-RF multi-user communication through reconfigurable intelligent surfaces: an information-theoretic analysis. 2021. ArXiv:2101.07556

133 Nayak S, Patgiri R. 6G: envisioning the key issues and challenges. 2020. ArXiv:2004.04024

134 Mursia P, Sciancalepore V, Garcia-Saavedra A, et al. RISMA: reconfigurable intelligent surfaces enabling beamforming for IoT massive access. IEEE J Sel Areas Commun, 2021, 39: 1072–1085

135 Xia S H, Shi Y M. Intelligent reflecting surface for massive device connectivity: joint activity detection and channel estimation. In: Proceedings of IEEE International Conference on Acoustics, Speech and Signal Processing, 2020. 5175–5179

136 Lu Y, Dai L L. Reconfigurable intelligent surface based hybrid precoding for THz communications. 2020. ArXiv:2012.06261

137 Ning B Y, Chen Z, Chen W R, et al. Channel estimation and transmission for intelligent reflecting surface assisted THz communications. In: Proceedings of IEEE International Conference on Communications (ICC), 2020. 1–7

138 Tekbıyık K, Kurt G K, Ekti A R, et al. Reconfigurable intelligent surface empowered terahertz communication for LEO satellite networks. 2020. ArXiv:2007.04281

139 Pan Y J, Wang K Z, Pan C H, et al. UAV-assisted and intelligent reflecting surfaces-supported terahertz communications. IEEE Wirel Commun Lett, 2021. doi: 10.1109/LWC.2021.3063365

140 Hashemi R, Ali S, Mahmood N H, et al. Average rate and error probability analysis in short packet communications over RIS-aided URLLC systems. 2021. ArXiv:2102.13363

141 Ndjiongue A R, Ngatched T, Dobre O A, et al. Re-configurable intelligent surface-based VLC receivers using tunable liquid-crystals: the concept. 2021. ArXiv:2101.02369

142 Yang L, Yan X Q, da Costa D B, et al. Indoor mixed dual-hop VLC/RF systems through reconfigurable intelligent surfaces. IEEE Wirel Commun Lett, 2020, 9: 1995–1999

143 Bai T, Pan C H, Han C, et al. Empowering mobile edge computing by exploiting reconfigurable intelligent surface. 2021. ArXiv:2102.02569

144 Hu X, Masouros C, Wong K K. Reconfigurable intelligent surface aided mobile edge computing: from optimization-based to location-only learning-based solutions. IEEE Trans Commun, 2021. doi: 10.1109/TCOMM.2021.3066495

145 Hashida H, Kawamoto Y, Kato N. Intelligent reflecting surface placement optimization in air-ground communication networks toward 6G. IEEE Wirel Commun, 2020, 27: 146–151

146 Ge L H, Dong P H, Zhang H, et al. Joint beamforming and trajectory optimization for intelligent reflecting surfaces-assisted UAV communications. IEEE Access, 2020, 8: 78702–78712